



## When Katrina hit California

Peter Gerstoft,<sup>1</sup> Michael C. Fehler,<sup>2</sup> and Karim G. Sabra<sup>1</sup>

Received 19 June 2006; revised 24 July 2006; accepted 2 August 2006; published 8 September 2006.

[1] Beamforming of seismic noise recorded on 150 Southern California stations was used to identify body and surface waves generated by Katrina. Surface wave microseisms are commonly associated with oceanic storms; there are no previous comprehensive body wave observations. The temporal evolution of the surface and body waves was different, indicating a different source mechanism for the two wave types. The body-waves originated in shallow water east of New Orleans and propagated deep inside the Earth. The surface waves have source location that varies with frequency with the lowest frequency surface waves originating west of the hurricane track and the higher frequency ones to the east. The seismic observations are consistent with ocean wave hindcasts and provide clear association of microseism noise with storm activity. **Citation:** Gerstoft, P., M. C. Fehler, and K. G. Sabra (2006), When Katrina hit California, *Geophys. Res. Lett.*, *33*, L17308, doi:10.1029/2006GL027270.

### 1. Introduction

[2] Hurricane Katrina struck land on August 29, 2005 as one of the strongest in the United States. Katrina became a category 5 hurricane in the Gulf of Mexico at about 1200 UTC on the 28th, made landfall at 1100 UTC on 29th near the mouth of the Mississippi River, crossed Breton Sound, and made landfall again near the Mississippi-Louisiana border at 1500 UTC (see Figure 1a). The hurricane generated large ocean waves, which coupled energy into the Earth in the form of seismic waves. This seismic energy was detected at long ranges.

[3] Significant microseismic energy that originates in the oceans propagates as surface Rayleigh waves that can be observed over long distances [Haubrich and McCamy, 1969; Lacoss *et al.*, 1969; Dorman *et al.*, 1993; Friedrich *et al.*, 1998; Schulte-Pelkum *et al.*, 2004; Rhie and Romanowicz, 2004; Cessaro, 1994; Bromirski, 2001; Bromirski *et al.*, 2005]. For example, Schulte-Pelkum *et al.* [2004] reported seismic observations in Southern California of storms in the Pacific ocean. As observed in microseism spectra (0–5 Hz) [Webb, 1998], the majority of microseismic energy occurs at double the frequency of ocean swells (typical frequencies 0.1–0.2 Hz) and is termed double-frequency microseisms. A smaller amount occurs at the primary frequency of the ocean wave (typical frequencies 0.05–0.1 Hz) and is termed primary microseisms. P-waves from storms have only been observed in a few cases [Haubrich and McCamy, 1969] and not in the detail

reported here. P-wave energy attenuates proportional to distance squared whereas surface wave energy attenuates proportional to distance, making P-waves more difficult to observe for the same source level.

[4] In deep water, the pressure amplitude of the ocean waves decays exponentially with depth, and there is thus no significant coupling of ocean-wave energy at the primary frequency into seismic energy at the seafloor. Longuet-Higgins [1950] has shown that two ocean waves with the same frequency propagating in opposite directions in deep water interact nonlinearly to create a pressure distribution on the seafloor at twice the frequency of the waves. The nonlinearly generated wave couples into the seafloor creating propagating seismic waves.

[5] In shallow water, ocean waves interact directly with the seafloor and thus energy can be transferred to the Earth at the primary frequencies or multiples thereof. In analogy with rotating machinery that creates vibrations at multiples of the basic rotating frequency, shallow water waves can create seismic waves at higher multiples of the ocean wave frequency. While the precise mechanisms for the energy transfer between shallow-water ocean waves and seismic waves are not known it is expected that shoaling and breaking waves are the main causes.

[6] Ocean waves propagate much slower than seismic waves (typical ocean wave speed is 20–40 m/s while seismic wave speed is 3000–12000 m/s). Thus, with distant seismic sensors, it is possible to observe the ocean state in near-real time. We were not able to observe Katrina on time series from a single geophone in California, but beamforming using array data can be used to detect and localize the seismic waves thus allowing us to make inferences about the coupling of hurricane-generated ocean waves to seismic waves.

### 2. Approach

[7] Using continuous data recorded during the hurricane by 150 seismic stations in Southern California (in effect a large-scale array), we formed beams and determined the azimuth and slowness (inverse velocity) of the waves crossing the array as a function of frequency (inverse period) [Johnson and Dudgeon, 1993; Rost and Thomas, 2002]. The recent availability of continuously recorded data from arrays consisting of a large number of stations makes such analysis possible. The array geometry and inferred azimuths from the array for the surface wave (great circle path 90° and 100°) and the P-wave (direct path 100°) are shown in Figure 1a. The analysis approach used is as follows: On each 7-minute time series, large events (earthquakes) are removed by truncating signal amplitude above one standard deviation. The resulting time series are Fourier transformed into the frequency domain where signal amplitude for each station is normalized within frequency bands

<sup>1</sup>Marine Physical Laboratory, University of California, San Diego, La Jolla, California, USA.

<sup>2</sup>Los Alamos National Laboratories, Los Alamos, New Mexico USA.

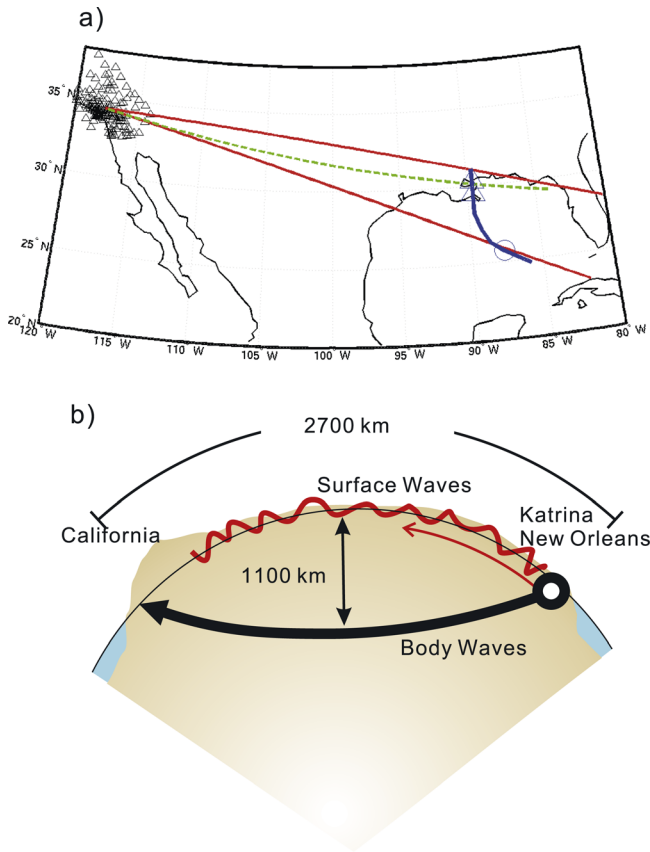


**Figure 1.** Propagation paths. (a) Stations (triangles) in the Southern California broadband seismic network. Bearings of  $90^\circ$  and  $100^\circ$  (red) from seismic array for surface waves and  $100^\circ$  for P-waves (green), track of Katrina (blue), along with location of where it became category 5 (circle) and landfalls (triangles) are indicated. (b) Schematic of the travel paths of observed wave types.

of width 0.002 Hz to equalize the contribution of each station to the beamforming. After beamforming, the slowness-azimuth beams are averaged across 5 frequency bins, giving a total frequency width of 0.01 Hz. Using the beamforming output and assuming a homogenous earth, we search for azimuth and slowness (inverse velocity) of an incoming wave. For a 0.1-Hz frequency and phase speed of 3 km/s the array beam width was  $4.5^\circ$ , giving a resolution in the Gulf of Mexico area of about 250 km in the radial direction relative to the array. Further, the azimuth and slowness can be biased due to inhomogeneous velocity structure and array bias. We will show that we are able to observe both surface and P-waves as indicated in Figure 1b.

[8] For each frequency analyzed, we searched for the combination of phase slowness and azimuth that gave the best fit to the data. For example, at a frequency of 0.07 Hz (Figure 2a) we find a wave having phase slowness of 0.30 s/km (velocity of 3.3 km/s) coming from  $98^\circ$  corresponding to a possible location of just south of New Orleans. This phase slowness corresponds to a surface wave. The body P-wave is observed at higher frequencies, e.g., 0.19 Hz (vertical component Figure 2b and horizontal radial component Figure 2c), also coming from  $98^\circ$  and with a horizontal phase slowness 0.085 s/km (velocity of

11.7 km/s). Since the P-wave is propagating nearly vertically when impinging on the array, it is much stronger on the vertical component (Figure 2b, 7 dB above the noise floor) than on the radial horizontal component (Figure 2c, 3 dB above the noise floor and less localized). The P-wave was not observed on the transverse component. (The horizontal components can be rotated using the azimuth determined from vertical component). The P-wave arrives from a narrower set of azimuths than the surface wave. Further, the P-wave showed no dispersion, supporting the P-wave interpretation (see later). We observed no shear wave energy at any frequencies on the three-component data.

[9] Using travel-time tables, which show distance as a function of apparent velocity or travel-time for a P-wave [e.g., Kennett, 1995], we can estimate the distance to the source of the P-wave. Combining the estimated distances and azimuths, we map the loci of possible P-wave source locations, Figure 2d, which clearly shows the origin as being in the region of hurricane Katrina. The P-wave penetrates deep into the Earth and has a turning point at a depth of about 1100 km.

[10] Useful information can be obtained by tracking the maximum of the beamformer output for the surface and P-wave versus frequency (inverse period), see Figure 3, where we plot peak value and the corresponding azimuth and slowness. For the surface wave, we searched for slowness from 0.22–0.37 s/km and for P-wave from 0.05–0.15 s/km and all azimuths ( $0\text{--}360^\circ$ ) were searched. Based on the peak values and the stability of the corresponding slowness and azimuth, the surface wave is observed from 0.08–0.12 Hz, corresponding to the ocean wave frequency and the P-wave is observed in the 0.16–0.24 Hz interval, double the ocean wave frequency. It is observed that the P-wave shows no dispersion, whereas the surface wave shows dispersion, in agreement with expected Rayleigh wave propagation. In the next section, we will examine the time dependence of these observations.

### 3. Results

[11] The development of the storm can be understood by comparison with hindcast-modeling of the ocean wave field using observed ocean buoy data and wind field. Figure 4 (from Wavewatch III [Tolman, 2005]) shows four snapshots (0, 6, 12, 15 h UTC on 29 Aug) of significant ocean-wave height (Figure 4a) and dominant frequency of the spectrum (Figure 2b). Ocean waves are generated close to the track of the hurricane where the wind is strongest. The largest significant wave height is observed to the east of the track where the wind is strongest, as the wind direction and the forward motion of the hurricane are in the same direction [Young, 2003]. The ocean wave field can be seen moving slowly across the Gulf of Mexico. For example, the 0.05-Hz dominant frequency in Figure 4b is observed at  $t = 0$ h and then hits the Western shores at about  $t = 12$ h, indicating an ocean wave travel-time greater than 12 h. It can also be seen from Figure 4b that the eastern part of the Gulf is dominated by higher frequency waves. Contrary, the western part of the Gulf, with longer fetch and less wind, is dominated by low frequency (long-wave) swell.

[12] To assess correlations between the seismic wavefield and hurricane activity, we analyzed seismic data recorded in

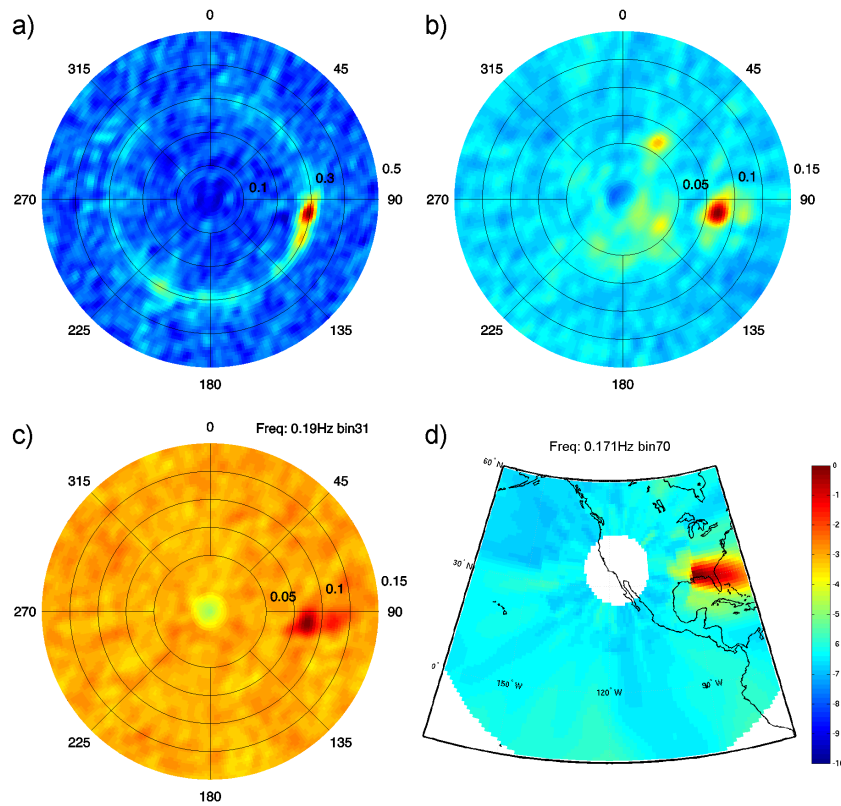


**Figure 2.** Beamforming and source region. (a) Azimuth-slowness map (dB) of the 0.07-Hz vertical component surface wave on 29 Aug. Phase slowness increases with radial distance from center of plot and ranges between 0–0.5 s/km. (b) Azimuth-slowness map of 0.19-Hz vertical component and (c) radial horizontal component body P-wave on 29 Aug. Slowness range is 0–0.15 s/km. (d) Source region of P-waves obtained by back-propagating using slowness and azimuth from beamforming in Figure 2b. All plots are shown on a 10-dB color scale normalized relative to the maximum peak.

Southern California during 7-minute intervals on 28–29 August and plot in Figure 5 the maximum beamformer output and the corresponding azimuth for both surface and P-wave as a function of time and frequency. In interpreting the figures note that it takes on the order of 10 min for the seismic energy to propagate from the Gulf of Mexico to California, whereas it can take several hours for the ocean waves to reach the shore, as can be seen in hindcasts from Wavewatch III [Tolman, 2005], see Figure 4.

[13] The prevailing direction for microseisms in Southern California is from the Pacific Ocean, about  $200^\circ$ , and in absence of Katrina, most energy would be coming from this azimuth. For example, the high beamformer output (Figure 5a) in the 0.12–0.14 Hz interval for the surface wave has an azimuth (Figure 5b) of about  $200^\circ$ . The strongest coherent surface wave energy (Figure 5a) is observed in the 0.06–0.1 Hz interval and based on the azimuth (Figure 5b) this stems from Katrina. The blue color in Figure 5b and 5d indicates azimuths from the Gulf of Mexico.

[14] Before landfall (1800 28 Aug to 1000 29 Aug), surface waves (Figure 5a) cross the network with azimuths ranging from  $85^\circ$  for the 0.1-Hz waves to  $105^\circ$  at 0.04 Hz, indicating that the source of the surface waves moves from east to west as frequency decreases. The azimuth from the array to the first landfall is  $95^\circ$ . Thus, higher frequency (shorter period) seismic waves originate to the east of the

hurricane and lower frequency (longer period) waves originate to the west. The spatial difference in surface wave origin is consistent with the hindcast in Figure 4b that shows that lower frequency ocean waves occur to the west of the hurricane and higher frequency waves to the east. The main frequency of the ocean waves is in the same interval as the surface waves and thus the surface waves are generated directly from the ocean waves. This is unusual as surface waves from microseisms are mainly observed at twice the frequency of the ocean waves [Haubrich and McCamy, 1969; Lacoss et al., 1969; Friedrich et al., 1998; Schulte-Pelkum et al., 2004; Rhee and Romanowicz, 2004; Cessaro, 1994; Bromirski, 2001]. As the hurricane makes landfall around 1100 UTC, the lower-frequency surface waves are no longer observed and the surface wave band compresses to 0.06–0.11 Hz (Figure 5b). These higher-frequency surface waves, which last until final landfall, have smaller azimuths (about  $85^\circ$ – $90^\circ$ ) indicating that they come from the coast NE of the hurricane track. The spatial and temporal variation in the surface wave source is remarkably consistent with the hindcast data in Figure 4. Finally, only during landfall do we observe surface waves in the double frequency interval 0.14–0.19 Hz.

[15] The body waves (Figures 5c and 5d) can be seen for nine hours after landfall. The time-frequency-azimuth plot for P-waves (Figure 5b) shows that these waves are initially

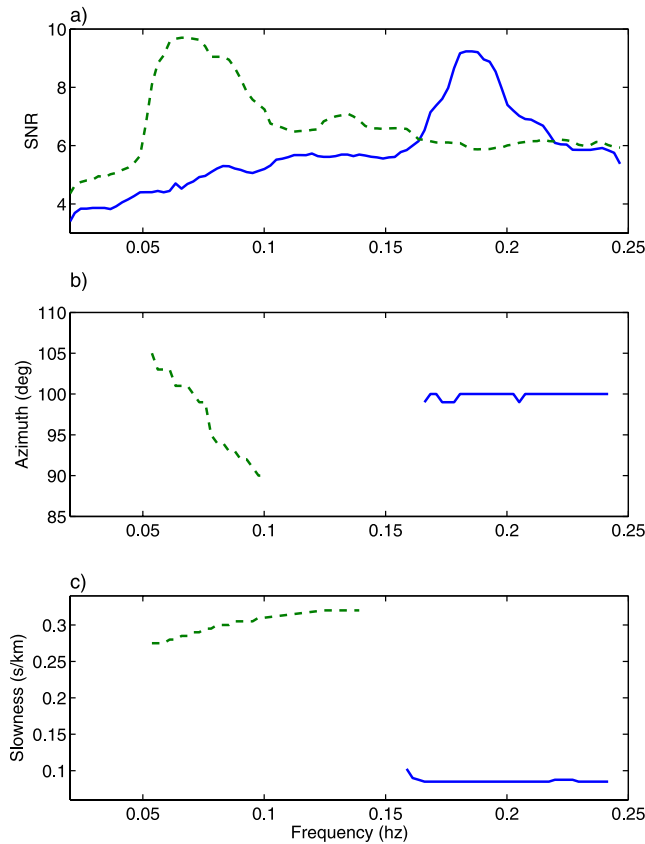


**Figure 3.** Beamformer output (a) at maximum for surface (dashed) and P (solid) at 10:00 on 26 Aug versus frequency displaying peak output (dB, above average output) and the corresponding (b) azimuth and (c) slowness. In Figures 2b and 2c only values corresponding to high peak output are shown.

(18h 28 Aug) centered at about a frequency of 0.19Hz, and the band widens with time until immediately before landfall when the azimuth from Gulf of Mexico covers the band 0.16–0.24 Hz (Figure 5d). The lower frequencies fade out first (see the time 18 h 29 Aug). The ocean-wave group speed decreases with frequency (inverse wave period) and the first ocean waves to hit the shore were generated while the hurricane was in the middle of the Gulf (Figure 4b) indicating that they had propagated for about half a day after their generation. Thus, one reason that the lower-frequency seismic body waves are observed first is that the lower frequency ocean waves propagate faster and thus arrive earlier into the shallow water regions where they couple energy into the solid earth, as observed for surface waves [Dorman *et al.*, 1993; Bromirski, 2001]. The observed azimuth of the P-waves (Figure 5d, see also Figure 3c) is constant and independent of both time and frequency. This indicates that the P-wave origin is fairly localized and, as indicated in Figure 2d, the source region could fall anywhere from the point of landfall to the shores east of the hurricane track.

[16] Beam power corresponds to the maximum coherent energy in a given direction (a beam) so the spectra shown in Figures 5a and 5c are related to the power of the P-wave and

the surface wave. As can be seen the two wave types have about the same maximum signal to noise ratio. Since noise is fairly constant across the frequency band of analysis, the two wave types can be inferred to have about the same power in Southern California. However, the differing temporal evolution of the maximum beam power for the surface and P-wave indicates different source mechanism for the two wave types.

#### 4. Discussion and Conclusions

[17] Our analysis indicates that both surface and P-waves are generated in shallow water likely due to shoaling or breaking of waves. However, their generation mechanism differs since they have different frequency content (surface wave at the ocean wave frequency and P-wave at double the frequency), different observation time, and different source region. While exact mechanisms for coupling of ocean to seismic waves are not understood, our observations indicate that at double the ocean wave frequency, the ocean/Earth

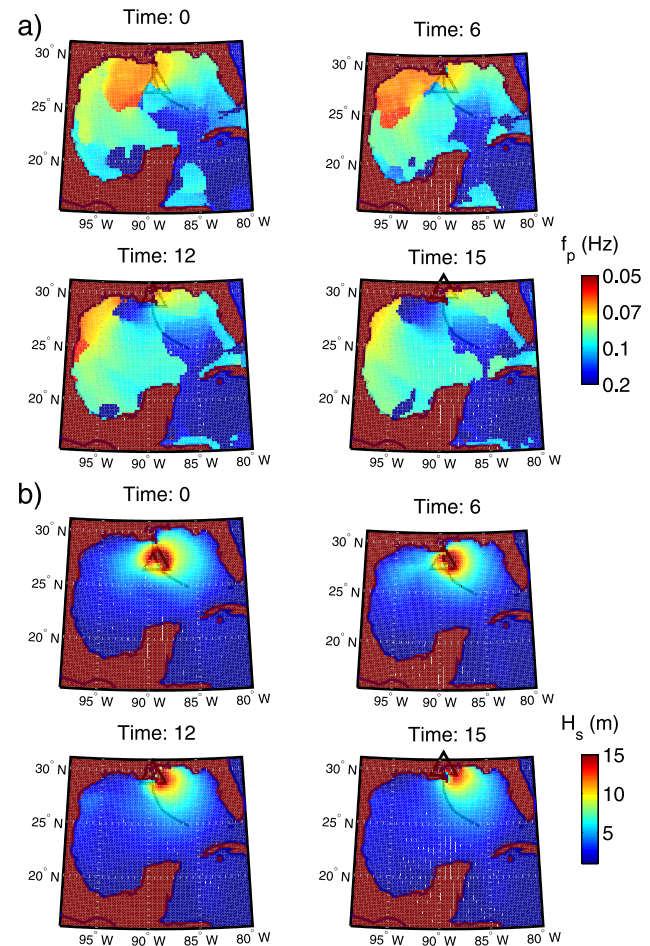


**Figure 4.** Ocean wave hindcast from Wavewatch III [Tolman, 2005]. (a) Peak ocean wave frequency and (b) significant wave height on 29 August at time 0, 6, 12, and 15 h UTC. The track of the hurricane (solid) and the eye of the hurricane at each observation time (triangle) are indicated.

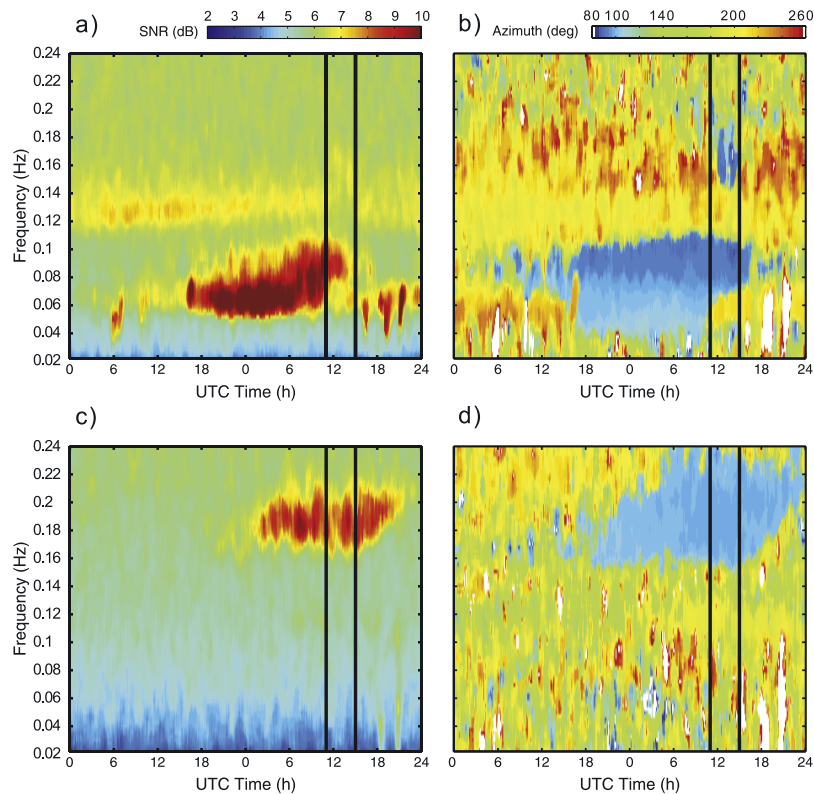


**Figure 5.** Peak of Beamformer for (a and b) surface wave and (c and d) P-wave versus observation time (28 and 29 August) and frequency. Peak output (Figures 5a and 5c) and the corresponding azimuth (Figures 5b and 5d) are displayed. Vertical lines ( $t = 11$  and  $15$ ) indicate the two landfalls. Peak output is measured in dB relative to the average output and only azimuth from  $80\text{--}260^\circ$  is shown.

interaction radiates more energy in the vertical direction and thus generates P-waves that propagate to long distances. In a previous observation of P-waves from storms [Haubrich and McCamy, 1969], these waves were also observed at double the ocean-wave frequency. They concluded that observed P-waves were generated in deep water due to the interaction of opposing ocean wavetrains [Longuet-Higgins, 1950]. The surface seismic waves at the dominant frequency of the ocean waves seem to be generated near the coast and the mechanism is likely due to interactions with the shallow seafloor or directly with the shoreline.

[18] The observed azimuths for the P-waves are constant and point in the direction towards the coast NE of the hurricane track and correspond to the region of highest observed ocean waves. In contrast, the surface waves are generated along the entire coast and the variation of the main frequency corresponds well with the variation of the ocean wave frequency obtained from the ocean wave hindcast.

[19] With the increased hurricane activity in the Gulf of Mexico, there is considerable interest in deploying more sensors (seismic, ocean acoustic, or infrasound) to better understand hurricanes. Seismic arrays are excellent at detecting low amplitude surface and body waves. We have demonstrated that body waves provide more information since both azimuth and slowness can be used for location. With these dense sensor arrays, it will be possible to observe and understand seismic signals from

storms at sea, and to track and better understand the sources of the seismic noise.

[20] **Acknowledgments.** Funding was provided by the UCSD/LANL CARE-program. Data were from the Southern California Earthquake Data Center, [www.data.sceec.org](http://www.data.sceec.org).

## References

- Bromirski, P. D. (2001), Vibrations from the “perfect storm”, *Geochem. Geophys. Geosyst.*, 2(7), doi:10.1029/2000GC000119.
- Bromirski, P. D., F. K. Duennebieber, and R. A. Stephen (2005), Mid-ocean microseisms, *Geochem. Geophys. Geosyst.*, 6, Q04009, doi:10.1029/2004GC000768.
- Cessaro, R. K. (1994), Sources of primary and secondary microseisms, *Bull. Seismol. Soc. Am.*, 84, 142–148.
- Dorman, L. M., A. E. Schreiner, L. D. Bibee, and J. A. Hildebrand (1993), Deep-water seafloor array observations of seismo-acoustic noise in the eastern Pacific and comparisons with wind and swell, in *Natural Physical Sources of Underwater Sound*, edited by B. Kerman, pp. 165–174, Springer, New York.
- Friedrich, A., F. Kruger, and K. Klinge (1998), Ocean-generated microseismic noise located with the Grafenberg array, *J. Seismol.*, 2, 47–64.
- Haubrich, R. A., and K. McCamy (1969), Microseisms: Coastal and pelagic sources, *Rev. Geophys.*, 7, 539–571.
- Johnson, D. H., and D. E. Dudgeon (1993), *Array Signal Processing: Concepts and Techniques*, Prentice-Hall, Upper Saddle River, N. J.
- Kennett, B. L. N., (1995), Seismic traveltime tables, in *Global Earth Physics: A Handbook of Physical Constants*, AGU Reference Shelf Ser., vol. 1, edited by T. J. Ahrens, pp. 126–143, AGU, Washington, D. C.
- Lacoss, R. T., E. J. Kelly, and N. M. Toksoz (1969), Estimation of seismic noise structure using arrays, *Geophysics*, 34, 21–38.
- Longuet-Higgins, M. S. (1950), A theory of origin of microseisms, *Philos. Trans. R. Soc. London, Ser. A*, 243, 1–35.

- Rhic, J., and B. Romanowicz (2004), Excitation of Earth's continuous free oscillations by atmosphere-ocean-seafloor coupling, *Nature*, *431*, 552–556.
- Rost, S., and C. Thomas (2002), Array seismology: Methods and applications, *Rev. Geophys.*, *40*(3), 1008, doi:10.1029/2000RG000100.
- Schulte-Pelkum, V., P. S. Earle, and F. L. Vernon (2004), Strong directivity of ocean-generated seismic noise, *Geochem. Geophys. Geosyst.*, *5*, Q03004, doi:10.1029/2003GC000520.
- Tolman, H. L. (2005), Manual and wave user system documentation of WAVEWATCH-III, ver. 2.22, 133 pp., U.S. Dep. Comm., Washington, D. C. (Available at <http://polar.ncep.noaa.gov/waves/wavewatch/wavewatch.html>)
- Webb, S. C. (1998), Broadband seismology and noise under the ocean, *Rev. Geophys.*, *36*(1), 105–142.
- Young, I. (2003), A review of the sea state generated by hurricanes, *Mar. Struct.*, *16*, 201–218.
- 
- M. C. Fehler, LANL, PO Box 1663, MS D443 Bldg 1572 Room 108, Los Alamos, NM 87545, USA.
- P. Gerstoft and K. G. Sabra, Marine Physical Laboratory, University of California San Diego, NTV 4th Fl, 8820 Shellback Way, La Jolla, CA 92093-0238, USA. (gerstoft@ucsd.edu)